

Searching for gravitational waves from pulsars in binary systems: an all-sky search

S. van der Putten¹, H. J. Bulten¹, J. F. J. van den Brand¹, M. Hol trop²

¹Nikhef, Sciencepark 105, 1098 XG Amsterdam, The Netherlands

²Department of Physics, University of New Hampshire, Durham, N.H. 03824, USA

E-mail: sputten@nikhef.nl

Abstract. Non axisymmetrical neutron stars emit continuous gravitational waves. The periodicity of the system allows for the improvement of the signal-to-noise ratio by integrating the signal over time. Many of the known neutron stars are in binary systems and their orbital movement will Doppler-shift the signal. When performing an all sky-search for such systems the use of exact binary motion templates become unfeasible. The Doppler shifts causes the power in the signal to be spread out over a large enough frequency band so that the gain of integrating the signal over the observation time is negligible. Here, the principles of a new analysis method for LIGO and Virgo data, called the polynomial search, will be presented together with first tests on simulated data.

1. Introduction

Gravitational wave detectors like LIGO and Virgo have reached their design sensitivity and direct detection of gravitational waves may become possible in the near future. Non axial-symmetric rotating neutron stars, or pulsars (when they emit radio or X-ray pulses), are systems that emit gravitational waves. The strain wave amplitude from such a system is calculated to be [1]

$$h_0 = \frac{16\pi^2 G}{c^4} \frac{\epsilon I_{zz} f^2}{r} \approx 4.2 \times 10^{-27} \left(\frac{I_{zz}}{10^{38} \text{kg m}^2} \right) \left(\frac{10 \text{kpc}}{r} \right) \left(\frac{f}{100 \text{Hz}} \right)^2 \left(\frac{\epsilon}{10^{-6}} \right), \quad (1)$$

where ϵ represents the ellipticity of the neutron star, I_{zz} the z -component of the moment of inertia, f the rotation frequency of the neutron star, G and c are the gravitational constant and the speed of light, respectively.

Neutron stars can be found as either isolated objects or in a binary system. In the following we discuss a new data analysis method termed the polynomial search, that enables an all-sky search for gravitational waves from neutron stars in binary systems.

2. Motivation

Most of the current all-sky searches [2, 3, 4, 5, 6, 7] focus on isolated neutron stars. From the ATNF pulsar catalog [8] it appears that the majority of the known pulsars with rotational frequencies above 10 Hz are in binary systems (see Fig. 1). The corresponding gravitational wave amplitude scales with f^2 (Eq. 1). However, the Keplerian orbit of the pulsar will introduce

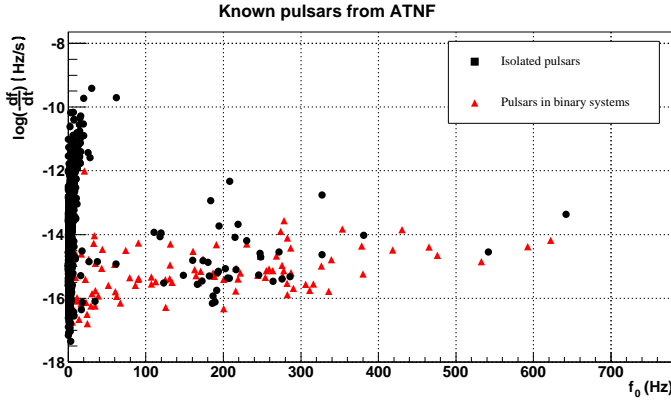


Figure 1. The spin versus the rotational frequency the down for isolated pulsars (black squares) and for pulsars in binary systems (red triangles). The data are taken from the ATNF pulsar catalog (June 2009) [8].

a Doppler shift to the signal in addition to the Doppler shift from the detector motion. These Doppler shifts cause the signal power to be spread out in frequency.

In order to take full advantage of the long integration times, templates must be matched with the data and they must be coherent with the signal over as long a time as possible. When attempting an all-sky coherent search for neutron stars in binary systems the number of required signal templates was found to be so large that such a search would be unfeasible [9].

Another strategy which is used in all-sky searches for isolated neutron stars is the Hough transform search [4]. This method uses shorter integration times so that the signal stays in a single frequency bin. When applying this principle to neutron stars in binary systems [9] one finds that the maximum coherent time for a signal T_{coh} to stay in one frequency bin can be written as

$$T_{coh} \leq 131.6 \left(\frac{(1+q)^{1/3}}{\sqrt{q}} \right) \left(\frac{P}{1 \text{ day}} \right)^{2/3} \left(\frac{m_{NS}}{1.4 M_{\odot}} \right)^{-1/6} \left(\frac{f}{1 \text{ kHz}} \right)^{-1/2} \text{ sec}, \quad (2)$$

where $q = m_2/m_{NS}$ represents the ratio of the masses of the two objects, P the period of the binary, m_{NS} the mass of the neutron star and f the gravitational wave frequency. For an example binary system with parameters $m_2 = m_{NS} = 1.4 M_{\odot}$, $P = 2 \text{ h}$ and $f_0 = 1 \text{ kHz}$ we find $T_{coh} \approx 20 \text{ s}$. This coherent time is too short to gain any significant signal to noise ratio by continuous observation.

The polynomial search is a hierarchical search that employs a limited number of filters and aims to increase the possible coherent time by more than an order of magnitude compared to the Hough transform search. Next, the first step of the hierarchical pipeline will be presented.

3. The polynomial search method

The Doppler shifts induced by the Kepler orbit of the neutron star will spread the signal over many frequency bins. The parameter space can be represented by the $12 + s$ dimensional vector

$$\vec{\lambda} = (P, a_p, e, \omega_0, h_0, \phi_0, \tau, f_0, \alpha_{ns}, \delta_{ns}, i, \psi, f^{(1)}, \dots, f^{(s)}),$$

where P represents the period of the binary, a_p the projected semi major axis, e the eccentricity of the orbit, ω_0 the longitude of the periastron, τ the time of periastron passage, h_0 the gravitational wave amplitude the signal has at the detector, ϕ_0 the initial phase of the gravitational wave, f_0

the rotation frequency of the neutron star, α_{ns} and δ_{ns} the right ascension and declination of the source, i the angle between the rotation and propagation axis, ψ the polarization angle of the gravitational wave and $f^{(1)}$ to $f^{(s)}$ the spin down parameters.

Instead of attempting to create templates in the $12 + s$ dimensional parameter space, the polynomial search employs the empirical phase model given by

$$\Phi(t; \vec{\xi}) = 2\pi \left(\phi_0 + f_0 t + \frac{\alpha}{2} t^2 + \frac{\beta}{6} t^3 \right), \quad (3)$$

where the vector $\vec{\xi} = (\phi_0, f_0, \alpha, \beta)$ lives in a four dimensional filter parameter space. This phase model has the advantage of a lower dimensionality of the parameter space and is a priori not dependent on any (astro)physical assumptions. However, the model will only hold as long as the coherent time is short enough or the Keplerian parameters are small enough in such a way that the phase from Eq. (3) does not deviate more than a certain value from the real signal. The filters

$$F(t; \vec{\xi}) = \sin(\Phi(t; \vec{\xi})) \quad (4)$$

are to be applied to the data in stretches of coherent time T . The maximal values for α and β can be calculated from the Kepler orbits assuming that the dominant contribution in the frequency dependence on time arises from the Doppler shifts. The values are calculated for a specific binary by taking the maximal values for the first and second derivatives for α_{max} and β_{max} .¹ For the previously introduced example binary, the values are $\alpha_{max} = 1.3 \text{ mHz/s}$ and $\beta_{max} = 1.1 \mu\text{Hz/s}^2$. Thus when applying the filters described in Eq. (4) and stepping in parameter space up to these maxima, all binary systems will be covered by these filters if the binary parameters lead to Doppler shifts smaller than the extreme case. The step size has been chosen by performing Monte-Carlo simulations assuming that the higher order corrections are small. The stepsize was chosen by computing the maximal distance of the true parameters to the nearest point in parameter space which results in a phase difference of $\pi/2$ for the complete filter. The details of these simulations will be presented in a future publication. The maximal coherent time, defined as the maximal time that the filter stays in phase within 1 radian with the original signal, can be calculated to be $T = 500 \text{ s}$ for this binary. Thus the polynomial search will gain a factor of 25 in coherent time over a Hough search.

The polynomial search is performed by stepping in the parameter space and creating a collection of filters. The filters are then applied to the data by calculating the correlation with the data $D(t)$ and each filter $F(t - \tau)$ where τ represents the lag parameter which can be interpreted as the time shift of the filter. This correlation C as a function of lag τ and filter with parameters $\vec{\xi}$ is computed in the frequency domain for computational efficiency which, when taking the noise level of the detector into account can be written as

$$C(\tau; \vec{\xi}) = \mathcal{F}^{-1} \left[\frac{\mathcal{F}[D(t)] \mathcal{F}[F(t; \vec{\xi})]^*}{\sqrt{2P_F S_n(\omega)}} \right], \quad (5)$$

where the operator $\mathcal{F}[\cdot]$ represents the operation of taking the Fourier transform, $*$ denotes the complex conjugate, $D(t)$ the data from the detector, $F(t; \vec{\xi})$ the filter with parameters $\vec{\xi}$, P_F the spectral power in the filter and $S_n(\omega')$ the single-sided power spectral density of the data, which is used to estimate the noise level of the detector. The resulting statistic can be considered Gaussian distributed with unit variance².

¹ In practice, the choice for α_{max} and β_{max} will determine the maximum span of the binary parameter space one would wish to search.

² In this case, the correlation C can also be interpreted as a signal to noise ratio as can be found with the Neyman-Pearson criterion

Eq. (5) gives the correlation for each filter with the data, shifted with lag parameter τ . The phase as a function of the lag can be written as

$$\Phi(t - \tau) = 2\pi \left[\underbrace{\left(\phi_0 - f_0\tau + \frac{\alpha}{2}\tau^2 - \frac{\beta}{6}\tau^3 \right)}_{\phi(\tau)} + \underbrace{\left(f_0 - \alpha\tau + \frac{\beta}{2}\tau^2 \right)}_{f_0(\tau)} t + \frac{1}{2} \underbrace{(\alpha - \beta\tau)}_{\alpha(\tau)} t^2 + \frac{1}{6}\beta t^3 \right]. \quad (6)$$

From Eq. (6) it can be seen that the lag parameter creates an interdependency of the filter parameters. This property can be exploited to avoid generating filters for each point in the parameter space which will reduce the amount of CPU time and memory needed. In order to use the lag parameter as a time shift it must be possible to shift the filter within the chunk of data between 0 and T s. In our implementation the filters are zero-padded for $t > T/2$ and only the lags $0 < \tau < T/2$ are considered.

The filters are produced in a frequency band Δf and are compared to the data by shifting the spectrum of the filter which is equivalent to heterodyning the data. When discretizing the filter $N = \Delta f T$ values of the correlation $C(\tau, \vec{\xi})$ for the lags between 0 and $T/2$ are obtained, where Eq. (6) shows the dependency of the parameters on the lag. In order to reduce the number of correlations to process, only the maximum correlation and corresponding values for τ , f_0 , α and β are recorded³ for each applied filter $F(t; \vec{\xi})$.

Since the correlation is normalized to the power spectral density, a threshold in terms of the estimated noise level of the detector can be set. When applying such a threshold to the collection of maxima the resulting numbers are called *hits*. These hits can be displayed by plotting the frequency as a function of time,

$$f(t - \tau) = \frac{1}{2\pi} \frac{d\Phi(t - \tau; \vec{\xi}_{hit})}{dt}, \quad (7)$$

where $\vec{\xi}_{hit}$ represents the parameters of the filters for which the correlation exceeds the threshold.

4. Sensitivity

The probability that, given a threshold and in absence of a signal, at least one filter will give a hit is called the false alarm probability. For the assumption of Gaussian noise and statistically independent filters, the false alarm probability can be written as

$$p_{fa}(x > x_{thr}) = 1 - \left(\frac{1 + \text{erf}(\frac{x_{thr}}{\sqrt{2}})}{2} \right)^{N_F}, \quad (8)$$

where x is the correlation of a single filter with parameters $\phi(\tau)$, $f_0(\tau)$, $\alpha(\tau)$ and $\beta(\tau)$ has with the data, x_{thr} the threshold normalized to the estimated noise level of the data and N_F is the total number of applied filters.

The false dismissal probability for a signal of a certain strength is defined as the probability that no correlation between filter and data passes a given threshold. The false dismissal probability for a given signal can be calculated if the correlations κ_i of all filters with the signal with amplitude h_0 and S_n are known. The expression is given by

$$p_{fd}(x < x_{thr}) = \prod_{i=0}^{N_F-1} \left(\frac{1 + \text{erf} \left(\frac{x_{thr} - \kappa_i \chi}{\sqrt{2}} \right)}{2} \right), \quad (9)$$

³ The value for ϕ_0 has been fixed to 0. Note, that by considering all lag parameters τ all values of $\phi(\tau)$ are sufficiently covered.

where and $\chi = h_0 \sqrt{\frac{T}{S_n}}$.

The false alarm and false dismissal rates are calculated for an example scan with parameters

$$T = 1200 \text{ s}, \Delta f = 8 \text{ Hz}, \alpha = \pm 10^{-3} \text{ Hz/s} \text{ and } \beta = \pm 10^{-5} \text{ Hz/s}^2,$$

where T represents the integration time, f_F the sample frequency of the filters, Δf the bandwidth of the data which has been used for the polynomial search, α and β give the range of both parameters which have been used in this search. For this particular set of parameters the amount of explicitly computed filters n_f is 10^5 . Using these parameters one finds that the number of distinct applied filters per Hz of searched data $N_F = N n_f = 1.2 \times 10^8$ filters/Hz.

The false alarm probability as a function of the threshold can be calculated directly with Eq. (8) and the number of applied filters. On the other hand the false dismissal probability depends on the value of the correlation of each filter with the signal. This means that the false dismissal probability can be estimated by using simulations.

The false dismissal probability was estimated for the parameters stated above. In the calculation of the false dismissal probability, only the filters which had $\kappa_i > 0.5$ were taken into account due to the large number of filters with smaller correlations. In this manner, the product in Eq. (9) runs over a subset of filters⁴ and the calculation of the false dismissal rate as a function of signal strength can be done in a timely manner.

Fig. 2 shows the false alarm (left panel) and false dismissal (right panel) probability per Hz as a function of the threshold and of χ , respectively. For a given signal strength $h = \chi \sqrt{\frac{T}{S_n}}$ and

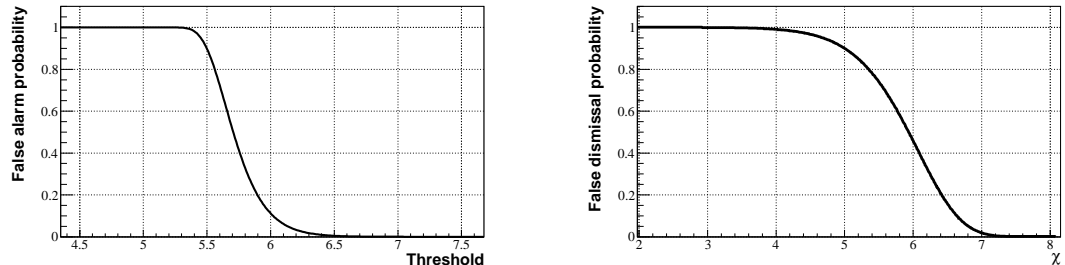


Figure 2. The left panel shows the false alarm probability per Hz searched bandwidth which has been computed using the parameters given in the text. The right panel show the false dismissal probability as a function of the signal strength. A threshold of 6.4, corresponding to a 1% false alarm probability has been used.

a given number of data chunks the probability for k hits in n data chunks is

$$P(k) = \frac{n!}{k!(n-k)!} p_{fd}^{n-k} (1 - p_{fd})^k, \quad (10)$$

where p_{fd} is the false dismissal probability as shown in Eq. (9) and in Fig. 2. The corresponding false alarm probability can be computed similarly.

5. Simulations

In order to illustrate the effectiveness of the polynomial search a binary system has been simulated with parameters

$$P = 0.1 \text{ d}, a_p = 2 \text{ ls}, e = 0.1, f_0 = 600 \text{ Hz}, h_0 = 10^{-27},$$

⁴ Of the 9.6×10^8 filters in the search band only about 500 have a $\kappa_i > 0.5$.

where P represents the period of the binary in days, a_p the projected semi major axis in light seconds, e the eccentricity of the orbit, f_0 the frequency of the gravitational wave emitted by the neutron star and h_0 the emitted amplitude of the gravitational wave. The beam pattern function of the interferometer has not been taken into account. The total simulation contained 6 hours of data sampled at 4 kHz and 35 overlapping FFTs (Fast Fourier Transforms) were made from this data. The polynomial search was performed with the parameters shown in the previous section.

Fig. 3 shows the frequency evolution of the signal in a time-frequency diagram where the color coding shows the strain of the signal. It can be seen that per FFT the power is spread

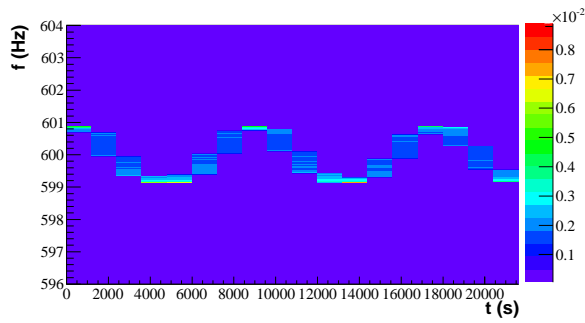


Figure 3. The frequency-time diagram of the simulated signal without noise.

out over a number frequency bins depending on the phase of the Keplerian orbit of the neutron star.

Gaussian noise has been added to the signal in the time domain with different amplitudes. The top left panel of Fig. 4 shows the frequency time diagram just like in Fig. 3 but with

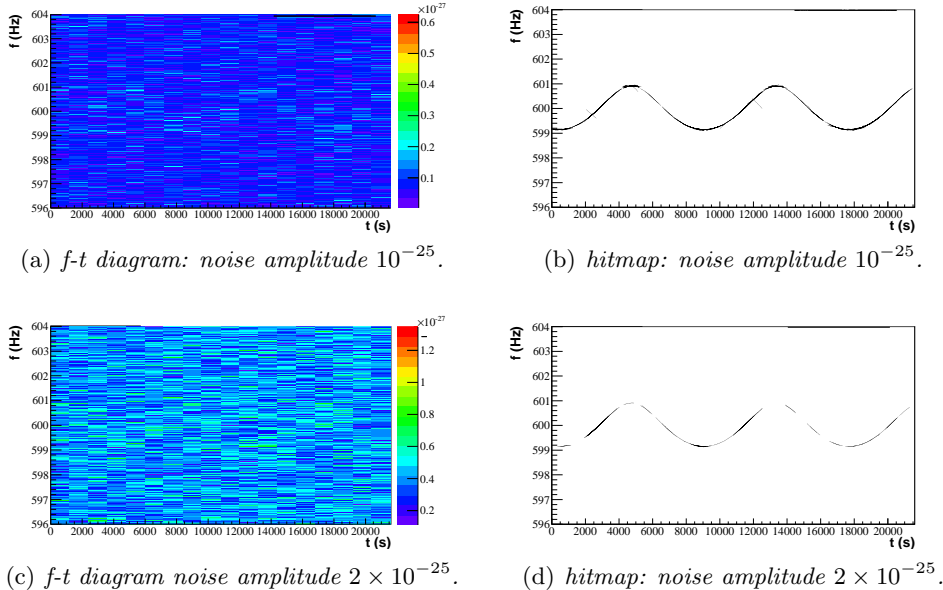


Figure 4. The frequency-time diagram of the simulated signal and the hit maps coming from the polynomial search which are made with a threshold of 6.4.

added noise with an amplitude of 10^{-25} in the time domain. Given the 1200 s coherent time⁵, this corresponds to a SNR in amplitude of 0.35. The top right panel shows the result of the polynomial search. This plot is made using the filters which exceed the threshold of 6.4. The filters are written in the form shown in Eq. (7) and drawn as a function of time.

The bottom left plot shows the same signal, but with a noise amplitude of 2×10^{-25} and bottom right shows the result coming from the polynomial search. Fig. 4 demonstrates the effectiveness of the polynomial search in terms of improved signal to noise ratio.

6. Conclusion and outlook

An algorithm for performing an all-sky search for gravitational waves from neutron stars in binary systems, called the polynomial search, has been presented and the first step in an hierarchical pipeline has been discussed. The polynomial search uses an empirical phase model which can describe the phase evolution up to third order in time, or the frequency evolution up to second order in time. Using this method, the Doppler shifts of the gravitational wave signals from neutron stars in binary systems can be dealt with and the coherent length of the individual data segments can be increased. The false alarm and false dismissal probability of the method have been presented giving a theoretical sensitivity of the search applied to a single stretch of data.

The sensitivity of any coherent continuous wave search scales as \sqrt{T} where T is the observation time for a single chunk of data. The coherent part of a Hough search demands that the change in frequency of the signal cannot exceed one frequency bin. The first step of the polynomial search enables the use of observation times more than a factor of 25 longer with respect to a Hough search for a single data stretch. This allows for a factor of 5 in signal to noise gain.

The polynomial search is designed for performing an all-sky search for gravitational waves coming from neutron stars in binary systems. It has been shown that the polynomial search can follow gravitational waves with high Doppler shifts and stay coherent for longer than 10^3 s. The polynomial search has been shown to be able to search a large volume of the parameter space with a limited set of filters. In the simulation discussed in this paper 1.2×10^8 filters per Hertz bandwidth of data were sufficient to cover all frequency derivatives up to $| \frac{df}{dt} | \leq 2$ mHz/s and $| \frac{d^2f}{dt^2} | \leq 10$ μ Hz/s². The resulting hitmaps demonstrate that the polynomial search is able to recover the phase evolution of the signal from a neutron star in a binary system.

The computation of the hitmaps is fast; the entire search of a band of 8 Hz of data took ≈ 5 CPUh. Since the software makes use of large computing infrastructures like the GRID, a search over all data and all frequencies up to 2 kHz can be performed in real-time with ≈ 100 nodes.

The polynomial search as presented in this paper will be applied to the LIGO and Virgo data in the future. Using the computed false alarm rates upper limits can be set on the gravitational wave emission from neutron stars in binary systems. Furthermore, the polynomial search will be extended with a second step that links the hits in the hitmaps together and fits the physical parameters to the resulting signal.

Acknowledgments

This work is part of the research programme of the Foundation for Fundamental Research on Matter (FOM), which is financially supported by the Netherlands Organisation for Scientific Research (NWO).

⁵ The SNR would increase with \sqrt{T} if the signal would stay in one bin. Since the Doppler shift prevents this, the SNR increase would be less than \sqrt{T}

References

- [1] Jaranowski P, Krolak A and Schutz B F 1998 *Physical Review D* **58** 063001
URL <http://link.aps.org/doi/10.1103/PhysRevD.58.063001>
- [2] Brady P R, Creighton T, Cutler C and Schutz B F 1998 *Phys. Rev. D* **57** 2101–2116
URL <http://link.aps.org/doi/10.1103/PhysRevD.57.2101>
- [3] Brady P R and Creighton T 2000 *Phys. Rev. D* **61** 082001
URL <http://link.aps.org/doi/10.1103/PhysRevD.61.082001>
- [4] Krishnan B, Sintes A M, Papa M A, Schutz B F, Frasca S and Palomba C 2004 *Phys. Rev. D* **70** 082001
URL <http://link.aps.org/doi/10.1103/PhysRevD.70.082001>
- [5] Mendell G and Wette K 2008 *Classical and Quantum Gravity* **25** 114044 (8pp)
URL <http://stacks.iop.org/0264-9381/25/114044>
- [6] Abbott B et al 2008 *Phys. Rev. D* **77** 022001
URL <http://prd.aps.org/abstract/PRD/v77/i2/e022001>
- [7] Abbott B et al 2009 *Phys. Rev. D* **79** 022001
URL <http://prd.aps.org/abstract/PRD/v79/i2/e022001>
- [8] Manchester R N, Hobbs G B, Teoh A and Hobbs M 2005 *AJ* **129**
URL <http://www.atnf.csiro.au/research/pulsar/psrcat/>
- [9] Dhurandhar S V and Vecchio A 2001 *Phys. Rev. D* **63** 122001
URL <http://link.aps.org/doi/10.1103/PhysRevD.63.12200>